Journal of Applied Mechanics and Technical Physics, Vol. 43, No. 4, pp. 617–621, 2002

NONLINEAR DEFORMATION AND STABILITY OF NONCIRCULAR CYLINDRICAL SHELLS UNDER INTERNAL PRESSURE AND AXIAL COMPRESSION

L. P. Zheleznov and V. V. Kabanov

UDC 629.7.023:539.3

Stability analysis of noncircular shells is performed with allowance for nonlinear subcritical deformation. Explicit expressions for the rigid displacements of elements of noncircular cylindrical shells are obtained and used to construct shape functions of an effective quadrilateral finite element of natural curvature. A finite-element algorithm for solving problems of nonlinear deformation and stability of shells is developed. Stability problem of an elliptic cylindrical shell is considered. The effect of the ellipticity and subcritical nonlinear deformation of the shell on the critical load is studied. Results obtained are compared with available experimental data.

1. Rigid Displacements of Finite Elements of Noncircular Cylindrical Shells. For rigid displacements of elements, the strain components vanish. Setting the linear components of the strain tensor, changes in curvature, and torsion equal to zero [1], we obtain the equations

$$\varepsilon_1 = u_x = 0; \tag{1.1}$$

$$\varepsilon_2 = k_2(v_\beta + w) = 0; \tag{1.2}$$

$$\varepsilon_3 = v_x + k_2 u_\beta = 0; \tag{1.3}$$

$$\chi_1 = w_{xx} = 0; \tag{1.4}$$

$$\chi_2 = k_2[k_2(v - w_\beta)]_\beta = 0; \tag{1.5}$$

$$\chi_3 = [k_2(v - w_\beta)]_x = 0. \tag{1.6}$$

Here u, v, and w are the tangential displacements and deflection, respectively, R and $k_2 = R^{-1}$ are the radius and curvature of the cross section, respectively, β is the angle between the normal to the cross-sectional contour and the b axis, and x is the longitudinal coordinate (Fig. 1). The subscripts x and β denote differentiation with respect to x and β, respectively.

We integrate Eqs. (1.1)–(1.6). From Eq. (1.5), we obtain

$$v = w_\beta + RC_5, \qquad C_5 = \text{const}. \tag{1.7}$$

Equation (1.2) yields

$$w = -v_\beta. \tag{1.8}$$

Combining (1.8) and (1.7), we obtain the equation

$$v_{\beta\beta} + v = RC_5. \tag{1.9}$$

The solution of Eq. (1.9) has the form

$$v = C_3 c + C_4 s + v_n, \qquad c = \cos\beta, \qquad s = \sin\beta, \tag{1.10}$$

where v_n is a particular solution of the inhomogeneous equation, which can be determined by the method of varied arbitrary constants C_3 and C_4. Let

$$v_n = C_3 c + C_4 s, \tag{1.11}$$

Chaplygin Siberian Aviation Institute, Novosibirsk 630051. Translated from Prikladnaya Mekhanika i Tekhnicheskaya Fizika, Vol. 43, No. 4, pp. 155–160, July–August, 2002. Original article submitted November 27, 2001; revision submitted January 28, 2002.

0021-8944/02/4304-0617 $27.00

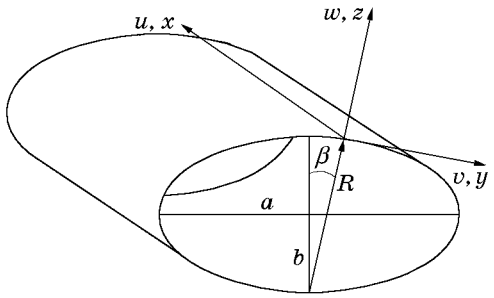

Fig. 1

where C_3 and C_4 are functions of x and β. Then, $v_{n\beta} = C_{3\beta}c - C_3 s + C_{4\beta}s + C_4 c$.

Assuming that

$$C_{3\beta}c + C_{4\beta}s = 0, \tag{1.12}$$

we obtain

$$v_{n\beta\beta} = -C_{3\beta}s - C_3 c + C_{4\beta}c - C_4 s.$$

In this case, Eq. (1.9) takes the form

$$C_{3\beta}s - C_{4\beta}c = -RC_5. \tag{1.13}$$

From Eqs. (1.12) and (1.13), it follows that

$$C_3 = C_5\psi_1 + C_7(x), \quad C_4 = -C_5\psi_2 + C_8(x), \quad \psi_1 = \int Rs\,d\beta, \quad \psi_2 = -\int Rc\,d\beta.$$

Equations (1.8), (1.10), and (1.11) can be combined to give $v = C_3 c + C_4 s - C_5(\psi_1 c + \psi_2 s) + C_7 c + C_8 s$ and $w = C_3 s - C_4 c - C_5(\psi_1 s - \psi_2 c) + C_7 s - C_8 c$. Condition (1.4) implies $C_7 = C_2 x$ and $C_8 = -C_1 x$. Then

$$\begin{aligned} v &= C_3 c + C_4 s - C_5(\psi_1 c + \psi_2 s) + (C_2 c - C_1 s)x, \\ w &= C_3 s - C_4 c - C_5(\psi_1 s - \psi_2 c) + (C_2 s + C_1 c)x. \end{aligned} \tag{1.14}$$

From Eq. (1.3), we obtain

$$u = C_1\psi_1 + C_2\psi_2 + C_6. \tag{1.15}$$

Functions (1.14) and (1.15) satisfy Eqs. (1.1)–(1.6) and, hence, describe displacements of elements as rigid bodies.

Let us consider the following particular cases:

— for *elliptic shells*, $z^2/b^2 + y^2/a^2 = 1$, $R = a^2b^2/d^3$, $d^2 = a^2s^2 + b^2c^2$, $\psi_1 = -b^2c/d$, and $\psi_2 = -a^2s/d$;

— for *parabolic shells*, $z^2 = 2py$, $R = p/c^3$, $\psi_1 = p/c^2$, and $\psi_2 = ps$;

— for *hyperbolic shells*, $z^2/b^2 - y^2/a^2 = 1$, $R = a^2b^2/d^3$, $d^2 = a^2s^2 - b^2c^2$, $\psi_1 = b^2c/d$, and $\psi_2 = -a^2s/d$;

— for *circular shells*, $z^2 + y^2 = R^2$, $\psi_1 = -Rc$, and $\psi_2 = -Rs$.

2. Finite Element and Algorithm of Solution. We construct shape functions of a quadrilateral finite element of natural curvature. Previously, similar elements were proposed for circular cylindrical shells and shells of revolution [2]. We divide a shell into m and n parts by the principal-curvature lines along the generatrix and directrix, respectively. Thus, the shell is modeled by $m \times n$ curvilinear rectangular finite elements. Approximating the tangential displacements and deflection by bilinear and bicubic functions, respectively, and taking into account (1.14) and (1.15), we write the total displacements of a finite element in the form

$$\begin{aligned} u &= a_1 xy + a_2 x + a_3 y + a_4 + a_6\psi_2 + a_{20}\psi_1, \\ v &= a_5 xy + a_6 xc + a_7 y + a_8(\psi_1 c + \psi_2 s) - a_{20} xs + a_{23} c - a_{24} s, \\ w &= a_9 x^3y^3 + a_{10}x^3y^2 + a_{11}x^3y + a_{12}x^3 + a_{13}x^2y^3 + a_{14}x^2y^2 + a_{15}x^2y + a_{16}x^2 + a_{17}xy^3 \\ &\quad + a_{18}xy^2 + a_{19}xy + a_{20}xc + a_{21}y^3 + a_{22}y^2 + a_{23}s + a_{24}c + a_6 xs + a_8(\psi_1 s - \psi_2 c). \end{aligned} \tag{2.1}$$

We write system (2.1) in matrix form

$$\tilde{\boldsymbol{u}} = P\boldsymbol{a}, \tag{2.2}$$

where $\tilde{\boldsymbol{u}} = \{u, v, w\}^{\mathrm{t}}$ is the displacement of the points of the middle surface of a finite element, $\boldsymbol{a} = \{a_1, \ldots, a_{24}\}^{\mathrm{t}}$ is the vector of unknown coefficients of the polynomials a_i, and P is a 3×24 matrix composed of the multipliers of the coefficients a_i in functions (2.1). Expressing the coefficients a_i in terms of nodal unknowns, we obtain

$$\boldsymbol{a} = B^{-1}\bar{\boldsymbol{u}}, \tag{2.3}$$

where $\bar{\boldsymbol{u}} = \{u_i, v_i, w_i, \vartheta_{1i}, \vartheta_{2i}, w_{xyi}, u_j, v_j, w_j, \vartheta_{1j}, \vartheta_{2j}, w_{xyj}, u_k, \ldots, w_{xyk}, u_n, \ldots, w_{xyn}\}^{\mathrm{t}}$ is the vector of nodal displacements, angles of rotations, and mixed derivatives of deflections, B is a 24×24 matrix whose nonzero elements have the form

$$b_{1,j} = p_{1,j}, \quad b_{2,j} = p_{2,j}, \quad b_{3,j} = p_{3,j}, \quad b_{4,j} = (p_{3,j})_x, \quad b_{5,j} = (p_{2,j} - (p_{3,j})_y)/R,$$

$$b_{6,j} = (p_{3,j})_{xy}\ (x = -a_1,\ y = -b_1), \quad b_{7,j} = p_{1,j}, \quad b_{8,j} = p_{2,j}, \quad b_{9,j} = p_{3,j}, \quad b_{10,j} = (p_{3,j})_x,$$

$$b_{11,j} = (p_{2,j} - (p_{3,j})_y)/R, \quad b_{12,j} = (p_{3,j})_{xy}\ (x = -a_1,\ y = b_1), \quad b_{13,j} = p_{1,j}, \quad b_{14,j} = p_{2,j},$$

$$b_{15,j} = p_{3,j}, \quad b_{16,j} = (p_{3,j})_x, \quad b_{17j} = (p_{2,j} - (p_{3,j})_y)/R, \quad b_{18,j} = (p_{3,j})_{xy}\ (x = a_1,\ y = -b_1),$$

$$b_{19,j} = p_{1,j}, \quad b_{20,j} = p_{2,j}, \quad b_{21,j} = p_{3,j}, \quad b_{22,j} = (p_{3,j})_x, \quad b_{23,j} = (p_{2,j} - (p_{3,j})_y)/R,$$

$$b_{24,j} = (p_{3,j})_{xy}\ (x = a_1,\ y = b_1), \quad j = 1, \ldots, 24, \qquad a_1 = L/(2m), \quad b_1 = l/(2n)$$

(L and l are the characteristic dimensions along the generatrix and directrix of the shell).

Substituting (2.3) into (2.2), we obtain the following relation between displacements of an element and nodal unknowns:

$$\tilde{\boldsymbol{u}} = PB^{-1}\bar{\boldsymbol{u}}.$$

There are six unknowns at each node and, hence, a finite element has 24 degrees of freedom. To determine the nodal unknowns, we use the Lagrange variational equation $\delta\Pi = 0$, where Π is the potential energy of the shell. We write the potential energy with allowance for nonlinear relations between strains and displacements [1]. The equation $\delta\Pi = 0$ leads to a system of nonlinear algebraic equations for nodal unknowns. The system is solved by the Newton–Kantorovich method. For a finite element, the equations have the form [3]

$$H\delta\bar{\boldsymbol{u}} = \boldsymbol{q}_e - \boldsymbol{G}, \qquad \bar{\boldsymbol{u}}^{n+1} = \bar{\boldsymbol{u}}^n + \delta\bar{\boldsymbol{u}},$$

where H is the Hess matrix of the finite element, determined from the second variation of the potential strain energy, $\boldsymbol{q}_e$ is the of nodal load vector, and $\boldsymbol{G}$ is the potential-energy gradient.

For the entire shell, the system of equations is constructed by a standard technique [4]. At each step of the iterative process, the system of linear algebraic equations is solved by decomposing the Hess matrix $H = L^{\mathrm{t}}DL$ [3], where L is a triangular matrix with unit diagonal and D is a diagonal matrix. The shell is stable if the second variation of the total potential energy of the shell is positive definite, which is equivalent to the positive defineteness of the Hess matrix. The latter is possible if all elements of the matrix D are positive. Therefore, we can confine our attention to the signs of the elements of the matrix D. The appearance of negative elements implies transition of the shell from a stable to an unstable state. Once the nodal unknowns are determined, we can calculate displacements and forces.

3. Nonlinear Deformation and Stability of an Elliptic Shell. We consider the problem of nonlinear deformation and stability of a simply supported cylindrical shell of elliptic cross section loaded by axial compressive force N and internal pressure p acting on the lateral surface of the shell. The shell has the length $L = 2800$ mm and thickness $h = 3.3$ mm. The radius of the shell $R_0 = 1000$ mm is determined as the radius of a circle with perimeter P equal to that of the ellipse:

$$R_0 = \frac{P}{2\pi} = \frac{2a}{\pi}\int\limits_0^{\pi/2} \Big\{1 + \Big[\Big(\frac{b}{a}\Big)^2 - 1\Big]\sin^2\psi\Big\}^{1/2} d\psi = \frac{2a}{\pi}\,\bar{E}\Big(\frac{\pi}{2}, \frac{b}{a}\Big).$$

Here $\bar{E}(\pi/2, b/a)$ is the complete elliptic integral of the second kind and a and b are the major and minor axes of the shell cross section, respectively. The shell is made of a material with Young's modulus $E = 7 \cdot 10^4$ MPa and

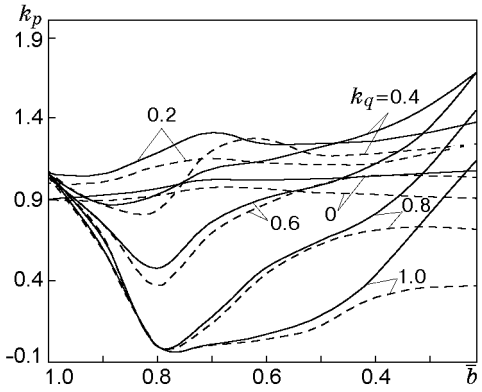

Fig. 2

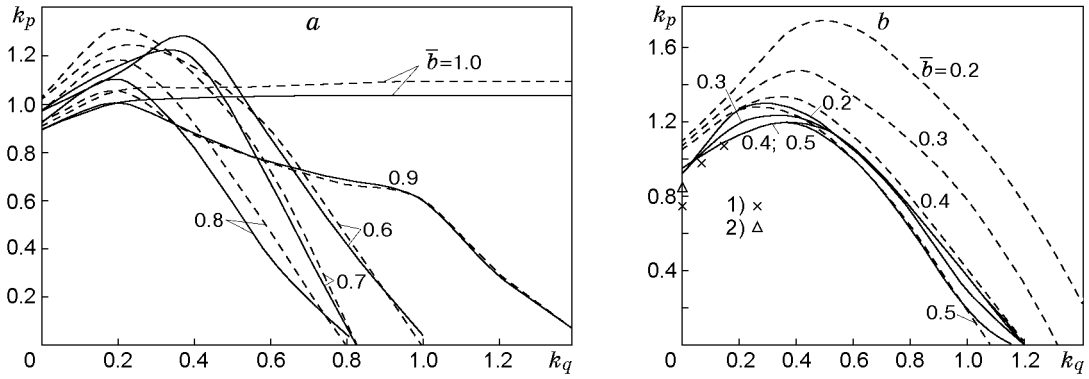

Fig. 3

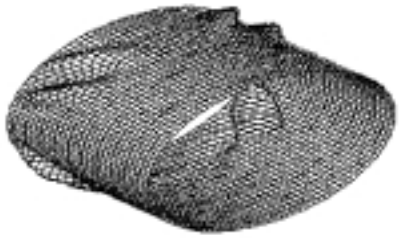

Fig. 4

Poisson's ratio $\nu = 0.3$. Konoplev and Kopp [5] obtained the following empirical formula for the critical internal pressure:

$$p_0 = \bar{p} E \gamma^2,$$

where $\bar{p} = (24.1\mu^{-1} + 130.2\mu^{-3} + 276.3\mu^{-5})\lambda^{-2}\gamma^{0.6}$, $\lambda = L/R_0$, $\gamma = h/R_0$, and $\mu = a/b$.

Figure 2 shows the parameter of the critical compressive force $k_p = N_{\rm cr}/N_b$ [$N_b = Eh^2/(R_b\sqrt{3(1-\nu^2)})$ and $R_b = a^2/b$] versus the ellipticity parameter $\bar{b} = b/a$ for linear and nonlinear initial stress–strain states (solid and dashed curves, respectively) for various values of the critical internal pressure parameter $k_q = p_{\rm cr}/p_0$. One can see from Fig. 2 that as $\bar{b}$ decreases, the critical load parameter first decreases (more rapidly for large k_q) and, then, increases. For $k_q < 0.4$, the parameter $\bar{b}$ affects results only slightly. The discrepancy between the corresponding curves is approximately 20%. As $\bar{b}$ decreases, the critical compressive load increases abruptly for the linear solution for $k_q > 0.4$, and in the case of nonlinear initial stress–strain state, the critical load is stabilized for $\bar{b} < 0.4$. For

almost all values of k_q and over the entire range of $\bar{b}$, the curves corresponding to the nonlinear solution lie below the corresponding curves for the linear solution. The exception is the shells for which $0.5 < \bar{b} < 0.8$ and $k_q = 0.4$. The effect of nonlinearity is more pronounced for $\bar{b} < 0.4$.

Figure 3 shows curves of k_p versus k_q for linear and nonlinear initial stress–strain states (solid and dashed curves, respectively) for various $\bar{b}$. One can see from Fig. 3 that as k_q increases, the critical load first increases slightly and reaches a maximum for $k_q = 0.2$, after which it decreases. The effect of the nonlinear stress–strain state becomes more pronounced as k_q increases. The discrepancy between the corresponding curves is 5–60%. Points 1 and 2 in Fig. 3b refer to the experimental data of [6, 7] ($\bar{b} = 0.5$).

Calculation results show that the stress–strain state and buckling mode of the shell are substantially nonuniform along both coordinates of the shell. A rhomb-like buckling mode occurs if the axial compression dominates. For low axial loads, oblique dents are formed. For other combinations of internal pressure and axial forces, a mixed buckling mode is observed. Figure 4 shows the buckling mode of a shell with $\bar{b} = 0.6$, $k_p = 0.2$, and $k_q = 0.9$.

The results were obtained using a 30×30 finite-element grid, which gives an error not larger than 5%. An octant of the shell was considered owing to symmetry.

REFERENCES

1. É. I. Grigolyuk and V. V. Kabanov, *Stability of Shells* [in Russian], Nauka, Moscow (1978).
2. A. I. Golovanov and M. S. Kornishin, *Introduction to the Finite-Element Method of Statics of Thin Shells* [in Russian], Kazan' Phys.-Tech. Inst, Acad. of Sci. of the USSR, Kazan' (1989).
3. S. V. Astrakharchik, L. P. Zheleznov, and V. V. Kabanov, "Nonlinear deformation and stability of shells and panels of nonzero Gaussian curvature," *Izv. Ross. Akad. Nauk, Mekh. Tverd. Tela*, No. 2, 102–108 (1994).
4. V. V. Kabanov and S. V. Astrakharchik, "Nonlinear deformation and stability of reinforced cylindrical shells under bending," in: *Spatial Structures in the Krasnoyarsk Region* (collected scientific papers) [in Russian], Krasnoyarsk (1985), pp. 75–83.
5. Yu. G. Konoplev and A. V. Kopp, "Experimental stability analysis of cylindrical shells of elliptic cross section," in: *Studies on the Theory of Plates and Shells* (collected scientific papers) [in Russian], Kazan' (1980), pp. 31–38.
6. L. V. Andreev, V. M. Kucherenko, and I. D. Pavlenko, "Stability of elliptic shells under axial load and lateral pressure," in: *Hydromechanics and Theory of Elasticity* (collected scientific papers) [in Russian], No. 29, 146–150 (1982).
7. R. C. Tennyson, M. Booton, and R. D. Caswell, "Buckling of imperfect elliptical shells under axial compression," *AIAA J.*, **9**, No. 2, 250–255 (1971).